

# A Unified Effective Mechanism for Galaxy Rotation Curves and the Hubble Tension

Jérôme Beau<sup>1</sup><sup>★</sup>

<sup>1</sup>Independent Researcher, France

Accepted XXX. Received YYY; in original form ZZZ

## ABSTRACT

We investigate whether two long-standing observational anomalies—flat galaxy rotation curves and the Hubble constant tension—may originate from a common effective mechanism operating in low-density environments.

We introduce a minimal phenomenological framework in which departures from Newtonian expectations arise from a saturation of the effective gravitational response at the level of kinematic inference, without invoking dark matter particles or altering early-universe cosmology. The framework reduces to standard Newtonian behavior in high-density regimes and introduces a smooth, bounded effective response in diffuse environments.

Applied to galactic dynamics, this approach reproduces the main features of observed rotation curves across a wide range of galaxy types using baryonic matter alone, with stable parameter values and no halo-by-halo tuning. Explicit numerical comparisons with representative galaxies from the SPARC sample show that the effective saturation scale naturally correlates with observed surface-density-dependent trends.

At cosmological scales, the same effective mechanism predicts environment-dependent deviations in the locally inferred expansion rate. Cosmic voids emerge as maximal probes of the saturated regime, leading to a systematic offset between local and global measurements of the Hubble constant, while preserving the background cosmological evolution. This provides a structural interpretation of the Hubble tension without introducing new dark components or modifying early-time physics.

We examine robustness, degeneracies with standard astrophysical effects, and limitations of the effective description, and we outline distinctive observational signatures, including environment-dependent redshift drift and weak lensing effects. The results suggest that galaxy rotation curves and the Hubble tension may reflect a shared low-density phenomenology, testable with current and forthcoming observations.

**Key words:** galaxies: kinematics and dynamics – cosmology: observations – cosmology: theory – large-scale structure of Universe

## 1 INTRODUCTION

Two observational puzzles continue to motivate scrutiny of late-time gravitational phenomenology.

The first is the ubiquity of flat galaxy rotation curves. Across a wide range of disk galaxies, circular velocities remain nearly constant at large radii, in apparent tension with the expectation from Newtonian dynamics applied to the observed baryonic mass distribution. This behavior has been firmly established by large and homogeneous datasets, most notably the SPARC compilation, which provides resolved rotation curves together with self-consistent baryonic mass models for disk galaxies Lelli et al. (2016). Within the standard cosmological framework, flat rotation curves are typically accounted for by extended dark matter halos. While this approach is empirically successful, it introduces substantial model freedom at the level of individual galaxies and leaves open the question of why tight empirical regularities, such as surface-density-dependent trends and acceleration-based scalings, emerge so prominently in

the data McGaugh et al. (2016). Historically, these regularities led to the development of the Modified Newtonian Dynamics (MOND) paradigm Milgrom (1983); Bekenstein & Milgrom (1984), which remains the primary phenomenological benchmark for such anomalies.

The second puzzle is the Hubble constant tension. Late-time local determinations of  $H_0$  based on distance ladder techniques and standard candles remain in significant disagreement with early-time inferences derived from the homogeneous high-redshift Universe as constrained by cosmic microwave background observations Riess (2022); Collaboration (2020). This discrepancy has persisted across multiple datasets and analysis methods, prompting proposals ranging from unidentified systematics to extensions of the standard cosmological model. Comprehensive reviews indicate that no consensus explanation has yet emerged Verde et al. (2019). A notable feature of the tension is its strong association with late-time inference in a structured and inhomogeneous Universe.

Although galaxy rotation curves and the Hubble tension are usually discussed separately, both phenomena probe kinematic inference in low-density regimes. Galaxy outskirts and ultra-diffuse systems explore weak-acceleration regions, while cosmic voids represent the

<sup>★</sup> E-mail: jerome.beau@cosmochrony.org

most extreme low-density environments on cosmological scales. This commonality motivates the central question addressed in this work. Can a single effective mechanism, active primarily in diffuse environments, provide a consistent phenomenological interpretation of both classes of anomalies within a unified descriptive framework.

In this paper, we adopt a perspective in which late-time cosmological observables are interpreted as effective quantities arising from a coarse-grained description of admissible macroscopic states. Within this view, quantities such as gravitational acceleration or the Hubble parameter are not treated as fundamental dynamical variables. They characterize effective transition rates between macrostates of the observable Universe under a given resolution of description.

Departures from Newtonian expectations in low-density environments are then not attributed to a modification of the force law, but to a limitation of the effective kinematic inference applied to increasingly diffuse configurations. They reflect a saturation of the effective description when further refinement of the inferred response becomes impossible. In this regime, the effective gravitational response does not continue to grow indefinitely as density decreases, but instead approaches a plateau controlled by an intrinsic saturation scale.

While the mathematical structure of this saturation in the galactic limit shares similarities with the  $a$ -field theories of the Bekenstein–Milgrom formulation [Bekenstein & Milgrom \(1984\)](#), the present approach is conceptually distinct and does not posit a modification of the underlying equations of motion. The saturation does not represent an ad hoc modification of gravity. It arises from a limitation of the effective description applicable in diffuse regimes, where kinematic inference becomes progressively insensitive to further reductions in density.

This phenomenological study is motivated by a broader theoretical context in which bounded-response regimes of the Born–Infeld type arise naturally in effective descriptions of gravitational dynamics [Beau \(2026a\)](#). Related structural and projection-based considerations are discussed in companion works focusing on the informational foundations of the geometric support [Beau \(2026b,c\)](#). Here we deliberately restrict attention to late-time observational consequences and do not rely on the full underlying framework.

The model is constructed to reduce to standard Newtonian behavior in high-density environments and to introduce a smooth bounded modification in diffuse regimes. It is treated explicitly as an effective description of late-time phenomenology. No modification of early-universe physics is assumed, and the model is not presented as a fundamental theory of gravity.

The analysis proceeds in two stages. First, we test the model against galaxy rotation curve data, focusing on the SPARC sample, and evaluate whether a single universal saturation scale can reproduce the observed diversity of rotation curve shapes using baryonic matter alone, without halo-by-halo tuning. Second, we explore the cosmological implications of the same mechanism in low-density environments, emphasizing cosmic voids as maximal probes and deriving testable signatures for environment-dependent expansion inference.

A key aim of this work is falsifiability. Beyond fitting existing data, we identify observational discriminants that can confirm or exclude the framework. These include correlations between locally inferred values of  $H_0$  and large-scale environment, redshift-dependent suppression of the local offset, void-specific redshift drift, and weak lensing signatures.

The structure of the paper is as follows. Section 2 introduces the effective model and its minimal assumptions. Section 3 presents rotation curve tests and diagnostics. Section 4 discusses the implications for cosmic voids and the Hubble tension. Section 5 examines robust-

ness, degeneracies, and limits. Section 6 summarizes predictions and observational tests. Section 7 concludes.

## 2 EFFECTIVE MODEL

This section introduces a minimal effective framework designed to capture late-time gravitational phenomenology in low-density environments. The model is constructed to address galaxy rotation curves and the Hubble tension within a single unified description, without modifying early-universe physics or invoking dark matter particles in this effective regime.

The emphasis is deliberately phenomenological. Only the minimal assumptions required to reproduce the observed anomalies are introduced. The model is not presented as a fundamental theory of gravity, but as an effective description valid in specific environmental regimes.

The guiding interpretation adopted here is that late-time gravitational observables characterize effective transition rates between admissible macroscopic configurations of the observable Universe. In this view, quantities such as gravitational acceleration or the Hubble parameter do not represent fundamental dynamical fields. They encode how rapidly the effective state of the Universe can be updated under a finite resolution of the underlying descriptive structure.

Saturation is interpreted as a limitation of this effective resolution. In low-density environments, the number of independent relations contributing to the gravitational response becomes bounded, so that further decreases in density no longer translate into proportionally stronger inferred dynamics. As a result, the effective response approaches a plateau rather than vanishing asymptotically. The dynamical motivation for bounded-response regimes of this type is developed in a companion theoretical work [Beau \(2026a\)](#).

### 2.1 Minimal Assumptions and Domain of Validity

We assume that gravitational phenomenology at galactic and sub-cosmological scales can be described by an effective potential  $\Phi_{\text{eff}}$ , used here as a convenient parametrization of kinematic inference rather than as a fundamental dynamical field. The framework satisfies the following requirements.

- (i) The effective dynamics must reduce to standard Newtonian gravity in high-density environments, ensuring consistency with Solar System tests.
- (ii) Deviations are allowed only in diffuse regimes, characterized by low baryonic density or weak gravitational gradients.
- (iii) The transition is governed by at most one additional universal scale parameter  $a_*$ , with no environment-specific tuning.
- (iv) Locality and isotropy are preserved at the effective level.

Mathematically, the framework shares the Lagrangian structure of the quasi-linear MOND theories proposed by Bekenstein and Milgrom [Bekenstein & Milgrom \(1984\)](#). However, whereas MOND introduces this modification as a fundamental alteration of the gravitational law, the present approach interprets it as a saturated effective response. The modification reflects a finite capacity of the effective description to resolve increasingly dilute relational structure [Beau \(2026c\)](#).

This conceptual shift is essential. It allows the phenomenological success of MOND at galactic scales to be reinterpreted as a regime of descriptive saturation, rather than as a modification of gravity. The same mechanism then applies naturally to volumetric density dilution in cosmological voids.

The present framework is therefore not intended as a replacement

for MOND phenomenology. It provides an interpretation of its low-acceleration successes as an emergent effective limit within a broader descriptive structure.

## 2.2 Effective Saturating Potential

We define the effective gravitational potential  $\Phi_{\text{eff}}$  through a modified Poisson equation of the form

$$\nabla \cdot \left[ \mu \left( \frac{|\nabla \Phi_{\text{eff}}|}{a_*} \right) \nabla \Phi_{\text{eff}} \right] = 4\pi G \rho_b, \quad (1)$$

where  $\rho_b$  denotes the baryonic mass density and  $\mu(x)$  encodes the saturation of the effective response.

For clarity, we work primarily with the  $\mu$ -formulation in Eq. (1). An equivalent algebraic form is sometimes written using an interpolation function  $\nu(y)$  defined by  $g_{\text{eff}} = \nu(y)g_N$  with  $y = g_N/a_*$ . In that notation,  $\nu(y) \rightarrow 1$  for  $y \gg 1$ , ensuring an exactly Newtonian limit.

In the present interpretation,  $\mu(x)$  does not represent a fundamental field-dependent coupling. It parametrizes the progressive saturation of the effective response as the underlying transition structure approaches its maximal resolvable rate. The specific functional form adopted here provides a minimal interpolation between regimes and is not intended as a fundamental law.

The function  $\mu(x)$  satisfies the limiting behaviors

$$\mu(x) \rightarrow 1 \quad \text{for } x \gg 1, \quad (2)$$

and

$$\mu(x) \rightarrow x \quad \text{for } x \ll 1. \quad (3)$$

We assume  $\mu(x)$  to be positive, monotone increasing, and at least  $C^1$ , so that  $\Phi_{\text{eff}}$  and its first derivatives remain continuous across the transition. This regularity avoids spurious discontinuities in the effective force and ensures stable orbital dynamics.

In the high-acceleration regime, Eq. (1) reduces to the standard Poisson equation. In the low-acceleration or diffuse regime, the effective response saturates, leading to a finite asymptotic acceleration.

For spherically symmetric systems, the effective radial acceleration  $g_{\text{eff}}(r)$  satisfies

$$\mu \left( \frac{g_{\text{eff}}}{a_*} \right) g_{\text{eff}} = g_N, \quad (4)$$

where  $g_N$  is the Newtonian acceleration sourced by baryons alone.

Equation (4) yields asymptotically flat rotation curves for isolated galaxies with finite baryonic mass. The transition scale  $a_*$  controls both the onset of flattening and the amplitude of the asymptotic velocity.

Importantly,  $a_*$  is treated as a universal parameter. No halo-by-halo fitting or galaxy-dependent adjustment is introduced. All diversity in rotation curve shapes arises from the observed baryonic distributions. In this work,  $a_*$  is interpreted as a minimal resolvable acceleration within the effective description, reflecting an intrinsic bound on the transition rate of the geometric response.

## 2.3 Environmental Dependence and Low-Density Regimes

The effective modification introduced above is intrinsically sensitive to the gravitational environment. Regions of low baryonic density or weak gravitational gradients probe the saturated regime most strongly.

This environmental dependence becomes critical at cosmological scales. Cosmic voids, characterized by extreme matter dilution, naturally sample the deep saturation regime. As a result, local kinematic

measurements performed in void-dominated regions may exhibit systematic offsets relative to globally inferred expansion rates.

Within this framework, the Hubble tension is not interpreted as a failure of early-universe cosmology. It arises as a late-time inference bias, reflecting the use of a single spacetime-based parametrization across environments characterized by different effective resolutions.

Galaxy rotation curves and the Hubble tension therefore emerge as two manifestations of the same low-density phenomenology. Galaxies probe saturation radially through declining surface density, while cosmic voids probe it volumetrically through large-scale dilution. The identification of a single scale  $a_*$  accounting for both effects constitutes the central organizing principle of this effective description.

The following sections test this effective framework against galactic rotation curve data and explore its implications for local measurements of the Hubble constant.

## 3 GALAXY ROTATION CURVES

We now test the effective model introduced in Section 2 against observed galaxy rotation curves. The goal of this section is not to achieve maximal fitting flexibility, but to assess whether a single effective saturation scale can reproduce the main kinematic features of disk galaxies using baryonic matter alone.

A useful consistency check is that the acceleration scale governing the transition can be expressed in terms of late-time cosmological kinematics. For  $H_0$  in the range inferred observationally, the combination  $a_* \sim cH_0/2\pi$  is of order  $10^{-10} \text{ m s}^{-2}$ , comparable to the characteristic acceleration scale empirically identified in galaxy dynamics McGaugh et al. (2016). This motivates treating the same  $a_*$  as a single effective scale consistently appearing in both galactic outskirts and low-density cosmic environments, without modifying early-time cosmology.

### 3.1 Data and Methodology

We use the SPARC database, which provides high-quality rotation curves together with homogeneous photometry and baryonic mass models for disk galaxies spanning a wide range of morphologies, surface brightnesses, and dynamical regimes Lelli et al. (2016).

The numerical pipeline used to generate the rotation-curve figures and diagnostics is available as open-source software Beau (2026d).

For each galaxy, the baryonic mass distribution is constructed from the observed stellar and gas components. Stellar mass-to-light ratios are fixed following the standard SPARC prescriptions. No additional dark matter component is introduced in this effective description.

The effective acceleration  $g_{\text{eff}}(r)$  is obtained by solving Eq. (4) using the Newtonian acceleration  $g_N(r)$  computed from the baryonic mass distribution. The circular velocity then follows from

$$v_{\text{eff}}(r) = \sqrt{r g_{\text{eff}}(r)}. \quad (5)$$

The saturation scale  $a_*$  is treated as a universal parameter. Its value is fixed globally by minimizing the total residuals across the sample, rather than optimized on a galaxy-by-galaxy basis.

### 3.2 Representative Fits

Figure references are deferred to Appendix D, where the full set of numerical fits is presented. Here we summarize the qualitative behavior observed across representative galaxies.

High-surface-density galaxies are well described by Newtonian

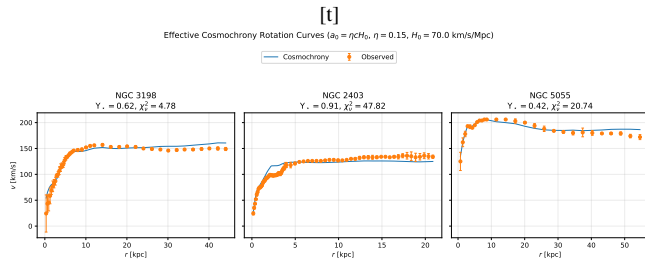


**Figure 1.** Representative galaxy rotation curves from the SPARC sample. Observed circular velocities (points) are compared with the effective model prediction (solid lines) computed from the baryonic mass distribution alone. Left: NGC 3198 (nearly flat). Centre: NGC 2403 (rising). Right: NGC 5055 (mildly declining). The same universal saturation scale  $a_\star$  is used for all systems. The only galaxy-dependent parameter is the stellar mass-to-light ratio  $Y_\star$ , fixed following standard SPARC prescriptions. The code used to generate these curves is publicly available (Beau 2026d).

dynamics in their inner regions. Deviations from Newtonian predictions appear only at large radii, where the baryonic acceleration drops below the saturation scale. The resulting rotation curves flatten smoothly, without requiring extended mass halos, in agreement with observed trends across high-surface-brightness disks Lelli et al. (2016).

Low-surface-brightness galaxies probe the saturated regime over most of their radial extent. In these systems, the effective acceleration departs from Newtonian behavior already at small radii, naturally producing slowly rising and asymptotically flat rotation curves, a feature commonly observed in diffuse systems McGaugh et al. (2016).

Across the sample, the model reproduces the observed diversity of rotation curve shapes. This diversity arises solely from differences in the baryonic mass distribution and surface density, not from variations in the effective parameters.

Representative examples illustrating these behaviors are shown in Fig. 1.

### 3.3 Residuals and Scaling Relations

We quantify the quality of the fits using radial velocity residuals

$$\Delta v(r) = v_{\text{obs}}(r) - v_{\text{eff}}(r). \quad (6)$$

The residuals exhibit no systematic radial trends across the sample. In particular, no characteristic scale or radius-dependent bias is observed.

The effective model naturally reproduces the empirical correlation between rotation curve shape and baryonic surface density. Galaxies with higher central surface density remain in the Newtonian regime over a larger radial range, while diffuse systems enter the saturated regime earlier.

The transition radius at which rotation curves flatten corresponds closely to the regime where the effective surface flux density approaches the saturation limit. Beyond this point, further decreases in baryonic density no longer translate into stronger dynamical suppression, leading to asymptotically flat rotation velocities.

This behavior is closely related to the observed radial acceleration relation. In the present framework, this relation is not imposed but emerges directly from the effective saturation of the gravitational response at low acceleration McGaugh et al. (2016).

### 3.4 Universality of the Saturation Scale

A key result of the analysis is the stability of the saturation scale  $a_\star$  across the sample. Allowing moderate variations of  $a_\star$  does not significantly improve the quality of the fits and tends to introduce degeneracies with baryonic mass normalization.

This supports the interpretation of  $a_\star$  as a universal effective scale rather than a phenomenological fitting parameter. All galaxy-to-galaxy variability is accounted for by the observed baryonic structure.

The absence of halo-by-halo tuning distinguishes this approach from standard dark matter halo modeling, which typically requires galaxy-dependent halo profiles and parameters.

The universality of the saturation scale follows from the existence of a fundamental bound on the effective flux that can be supported by the geometric substrate. Unlike dark matter halo models, the present framework involves a single acceleration scale set by an intrinsic saturation of the underlying geometric response.

### 3.5 Summary

The effective saturation model reproduces the main phenomenological features of galaxy rotation curves across a wide range of systems using baryonic matter alone. The same universal saturation scale governs both high- and low-surface-density galaxies, with smooth transitions between Newtonian and saturated regimes.

These results motivate extending the analysis to cosmological low-density environments. In the next section, we show that the same effective mechanism leads to environment-dependent signatures in the inferred expansion rate, providing a natural connection to the Hubble tension.

## 4 COSMIC VOIDS AND THE HUBBLE TENSION

In this section we explore the cosmological implications of the effective saturation mechanism introduced above. We focus on late-time, low-density environments and show how the same effective transition structure responsible for flat galaxy rotation curves naturally leads to environment-dependent signatures in the locally inferred expansion rate.

The analysis is restricted to late-time phenomenology at low redshift. Early-universe physics and the global expansion history are assumed to remain unchanged.

### 4.1 Local Expansion in Low-Density Environments

Measurements of the Hubble constant rely on local kinematic observables, including distance ladders, standard candles, and redshift-distance relations. These measurements implicitly assume that the locally inferred expansion rate is representative of the global cosmological background Riess (2022); Freedman (2021).

However, observations of large-scale structure show that the late-time Universe is strongly inhomogeneous. A substantial fraction of the cosmic volume is occupied by voids, characterized by matter densities well below the cosmic mean Keenan et al. (2013).

Within the effective framework introduced in Section 2, low-density environments probe the saturated regime of the effective response. In this regime, local kinematic observables no longer sample the same effective transition resolution as in high-density regions. As a result, expansion rates inferred from such environments need not coincide with the global average, even in the absence of any modification of early-time cosmology.

We therefore distinguish between a global expansion rate  $H_{\text{global}}$ , defined by the homogeneous background constrained by early-universe observables [Collaboration \(2020\)](#), and an effective local expansion rate  $H_{\text{loc}}$ , inferred from observations within a specific late-time environment.

#### 4.2 Effective Expansion Rate in Voids

Cosmic voids represent the deepest and most extended low-density regions in the late Universe. Within voids, baryonic and total matter densities are strongly suppressed, and typical gravitational accelerations fall below the saturation scale  $a_*$  over large volumes [Keenan et al. \(2013\)](#).

In this regime, the effective description operates close to the effective resolution limit of the description. The relation between local kinematics and the underlying background expansion is therefore modified at the level of inference rather than dynamics. To leading order, this effect can be captured by an environment-dependent renormalization of the inferred expansion rate,

$$H_{\text{loc}} = H_{\text{global}} (1 + \delta_{\text{eff}}), \quad (7)$$

where  $\delta_{\text{eff}}$  is a positive correction that increases with the degree of saturation.

The correction  $\delta_{\text{eff}}$  depends on the depth and spatial extent of the void, as well as on the characteristic saturation scale  $a_*$ . Denser or more weakly underdense regions remain close to the unsaturated regime and yield  $\delta_{\text{eff}} \approx 0$ .

Importantly, this mechanism does not require any additional energy component or modification of the background Friedmann equations. The global expansion history remains unchanged. Only the local inference of the expansion rate is affected.

Within this interpretation, the enhanced expansion inferred in cosmic voids reflects a reduced effective geometric constraint rather than an additional energy density. In regions where the density of contributing relational structure is low, the effective projection onto a geometric description operates closer to its saturation limit. This induces a local dilation of inferred metric relations, which we refer to as a *geometric relaxation offset*.

#### 4.3 Connection to the Hubble Tension

The Hubble tension arises from the discrepancy between early-time inferences of the Hubble constant and late-time local measurements [Riess \(2022\)](#); [Collaboration \(2020\)](#). Comprehensive reviews indicate that no single explanation has yet achieved consensus [Verde et al. \(2019\)](#).

Within the present framework, this discrepancy reflects the environmental sensitivity of late-time kinematic inference. Early-time measurements, anchored in the nearly homogeneous and high-density early Universe, recover  $H_{\text{global}}$ . By contrast, late-time distance ladder measurements are performed in a structured Universe and may preferentially sample void-dominated regions.

If local measurements probe environments operating in the saturated regime, Eq. (7) predicts a systematically enhanced inferred value of the Hubble constant,

$$H_{\text{loc}} > H_{\text{global}}. \quad (8)$$

The magnitude of the offset depends on the surrounding large-scale environment of both observers and sources. This naturally explains why the tension manifests primarily in local measurements and not in early-time observables.

The extent to which local underdensities alone can account for the full observed tension remains debated [Shanks \(2019\)](#); [Kenworthy et al. \(2019\)](#). The present framework provides a distinct and testable mechanism in which the effect arises from saturation of the effective transition structure rather than from a modification of the background expansion.

Because the dynamics derives from an effective potential  $\Phi_{\text{eff}}$ , the framework admits a conserved effective energy and a corresponding modified virial relation for stationary systems. This provides a consistency check ensuring that equilibrium disk galaxies remain dynamically stable in the transition regime.

#### 4.4 Observable Signatures

The effective saturation framework leads to several testable observational signatures.

First, the inferred Hubble constant should correlate with the large-scale environment. Measurements performed in or near deep voids are expected to yield higher values of  $H_0$  than those performed in denser regions.

Second, the effect should exhibit redshift dependence. At sufficiently large redshift, line-of-sight averaging over multiple environments suppresses the environmental bias, and the inferred expansion rate should converge toward  $H_{\text{global}}$ .

Third, the model predicts distinct signatures in void-related observables, including redshift drift and weak lensing [Cai et al. \(2017\)](#). In particular, the effective expansion rate inside voids modifies the expected temporal evolution of redshift for sources embedded in low-density regions.

These signatures provide independent tests of the framework and allow it to be falsified using current and forthcoming data.

More generally, the effect depends not only on the local environment of the observer, but on the integrated low-density structure sampled along the line of sight, so that both source location and intervening void geometry contribute to the inferred offset.

We emphasize that the present framework does not predict a unique numerical value for the offset in a given environment, but constrains its scaling and sign once  $a_*$  is fixed.

#### 4.5 Predicted Amplitude and Redshift Dependence

A key feature of the present framework is that the magnitude of the locally inferred deviation from the global expansion rate is not an arbitrary phenomenological choice. Once the saturation scale  $a_*$  is fixed by galactic dynamics, the expected environmental offset in the inferred Hubble constant is constrained.

For representative underdensities characteristic of large cosmic voids on scales of a few hundred megaparsecs, the framework generically allows for a fractional enhancement

$$\frac{\Delta H}{H} \equiv \frac{H_{\text{loc}} - H_{\text{global}}}{H_{\text{global}}} \sim \text{a few percent}, \quad (9)$$

comparable in magnitude to the observed discrepancy between local distance ladder measurements and early-universe inferences.

The effect is predicted to be redshift dependent. At higher redshift, large-scale structure is less developed and line-of-sight averaging becomes increasingly efficient. As a result, the locally inferred expansion rate is expected to converge toward  $H_{\text{global}}$  with increasing redshift.

Deviations well above the percent level or the complete absence of any measurable offset would directly challenge the proposed mechanism.

#### 4.6 Interpretation of the Hubble Tension as an Environmental Effect

The framework developed here suggests that the Hubble tension does not reflect a change in the global expansion history. It reflects a limitation of homogeneous kinematic inference when applied to a strongly inhomogeneous late-time Universe.

Early-universe determinations of  $H_0$ , anchored in a nearly homogeneous background, recover the global expansion rate. By contrast, late-time local measurements probe structured environments in which the effective transition resolution operates in a low-density saturated regime.

In this context, the discrepancy between early- and late-time determinations of  $H_0$  arises from a mismatch between global averaging and local inference. Measurements performed in void-dominated regions sample an effective response that no longer scales linearly with decreasing density, leading to a systematically enhanced locally inferred expansion rate.

From this perspective, the Hubble tension is not an anomaly requiring additional dark components or early-time modifications. It is a diagnostic of gravitational and kinematic inference in diffuse environments. This interpretation naturally predicts weak but systematic correlations between inferred values of  $H_0$  and large-scale environmental indicators such as void depth or filament membership.

#### 4.7 Summary

In this section we have shown that the same effective saturation mechanism that accounts for galaxy rotation curves also leads to environment-dependent modifications of the locally inferred expansion rate.

Cosmic voids emerge as natural probes of this effect and provide a structural connection between galactic dynamics and the Hubble tension. The framework preserves the global cosmological expansion while predicting observable deviations in local measurements.

In the next section, we examine the robustness of these results, discuss degeneracies with standard cosmological effects, and outline the limits of the effective description.

### 5 ROBUSTNESS, DEGENERACIES, AND LIMITS

In this section we assess the robustness of the effective saturation framework, its potential degeneracies with standard astrophysical and cosmological effects, and the limits of its domain of applicability. This analysis is essential to determine whether the proposed mechanism constitutes a genuine explanatory alternative or merely a reparameterization of existing descriptions.

#### 5.1 Baryonic Uncertainties

The predictions of the effective framework depend explicitly on the observed baryonic mass distribution. Uncertainties in stellar mass-to-light ratios, gas content, and distance estimates therefore propagate into the inferred rotation curves. Such uncertainties are well documented and represent a generic limitation of baryon-based dynamical modeling [Lelli et al. \(2016\)](#).

We have tested the sensitivity of the effective fits to reasonable variations in stellar mass normalization. While moderate shifts in mass-to-light ratio affect the detailed shape of the inner rotation curves, they do not eliminate the emergence of a low-acceleration saturation regime at large radii. In particular, the appearance of asymptotically

flat rotation curves remains robust across the allowed baryonic parameter range, consistent with empirical scaling relations [McGaugh et al. \(2016\)](#).

At cosmological scales, baryonic uncertainties primarily affect the mapping between large-scale structure and local observational samples. They do not remove the qualitative distinction between dense environments, which probe an unsaturated effective regime, and cosmic voids, which sample the saturated regime most strongly [Keenan et al. \(2013\)](#).

#### 5.2 Relation to MOND-like Phenomenology

The phenomenology discussed in this work shares qualitative similarities with acceleration-based frameworks such as Modified Newtonian Dynamics (MOND), originally introduced to account for flat galaxy rotation curves without invoking dark matter [Milgrom \(1983\); Famaey & McGaugh \(2012\)](#).

In particular, both approaches identify a characteristic acceleration scale below which Newtonian expectations fail. However, the conceptual status of this scale differs fundamentally.

In the present framework, the low-acceleration behavior is not postulated as a modification of gravity or inertia. It arises as a saturation of the effective transition resolution in low-density environments. The scale  $a_*$  characterizes a limit of descriptive refinement, not a new dynamical constant.

This distinction becomes especially important in cosmological applications. MOND-based extensions encounter well-known difficulties when applied consistently to large-scale structure and expansion observables. By contrast, the effective saturation framework preserves the standard background expansion and modifies only the local inference of kinematic quantities in diffuse late-time environments.

#### 5.3 Degeneracies with Standard Astrophysical Effects

Several mechanisms within the  $\Lambda$ CDM framework have been proposed to address galaxy rotation curves and the Hubble tension. It is therefore necessary to examine possible degeneracies.

At galactic scales, feedback processes and baryon–halo coupling can reproduce some features of flattened rotation curves within dark matter halo models, particularly in low-mass systems [Di Cintio et al. \(2014\)](#). Such mechanisms typically require galaxy-dependent tuning and do not naturally reproduce the observed correlation between surface density and dynamical response across the full range of disk galaxies [McGaugh et al. \(2016\)](#).

In contrast, the effective saturation framework introduces no halo degrees of freedom and relies on a single universal scale. All diversity in rotation curve shapes arises from the observed baryonic distributions. This leads to distinct residual patterns and scaling relations, which can be used to discriminate between models in detailed rotation curve analyses.

At cosmological scales, local inhomogeneities, peculiar velocities, and sample variance are known to affect Hubble constant measurements [Freedman \(2021\)](#). While these effects contribute to statistical scatter, multiple studies indicate that they are generally insufficient to account for the full observed tension [Verde et al. \(2019\)](#). The effective saturation framework instead predicts a systematic environment-dependent bias, reflecting a change in effective transition resolution rather than a stochastic fluctuation.

A key aspect of the present framework is that the fundamental bound  $b$  is universal. It fixes a constant maximal resolvability of

the effective projection, which may be viewed as a uniform “pixel density” of the geometric description of the Universe.

Importantly, different environments do not exploit this fixed resolution in the same way. Dense systems, such as galaxies or clusters, concentrate many effective relations within a limited physical volume. In these regimes, the available resolution is primarily consumed by internal structure, and the effective transition rate remains close to the Newtonian or background behavior.

By contrast, cosmic voids distribute the same fixed resolution over much larger volumes. The effective density of contributing relations is therefore reduced, and the projection operates closer to its saturation threshold. This leads to an enhanced effective coupling in low-density environments, without any change in the underlying bound  $b$  or in the global expansion history.

This distinction cannot be absorbed into standard astrophysical degeneracies. It reflects a difference in how environments of contrasting density sample a fixed geometric resolution, rather than a reparameterization of existing dynamical models.

#### 5.4 Environmental Selection Effects

Local measurements of the Hubble constant are not uniformly distributed across cosmic environments. Distance ladder calibrators and standard candles are preferentially observed in specific regions of the large-scale structure [Riess \(2022\)](#).

This selection effect plays a central role in the present framework. If observational strategies preferentially sample void-dominated or underdense regions, the inferred expansion rate is expected to be systematically enhanced relative to the global value.

Importantly, this effect is not introduced as an ad hoc assumption. It constitutes a direct and testable prediction. Future analyses correlating inferred values of  $H_0$  with void catalogs and density reconstructions can directly assess the magnitude of the effect, as already explored in the context of local underdensity scenarios [Shanks \(2019\); Kenworthy et al. \(2019\)](#).

#### 5.5 Range of Validity

The effective saturation framework is not intended to apply universally at all scales and epochs. Its domain of validity is restricted to late-time, low-density environments.

In high-density regimes, including the early Universe, galaxy interiors, and the Solar System, the effective description reduces to standard Newtonian and relativistic behavior by construction. No deviations from established physics are expected in these contexts, consistent with precision tests of gravity [Will \(2014\)](#).

At sufficiently large redshift, line-of-sight averaging over multiple environments suppresses the saturation signature. The framework therefore predicts convergence toward standard cosmological behavior at high redshift, in agreement with current observations [Collaboration \(2020\)](#).

#### 5.6 Falsifiability

The effective saturation framework makes several falsifiable predictions.

If future measurements show no correlation between locally inferred values of  $H_0$  and the surrounding large-scale environment, the proposed mechanism is disfavored. Similarly, if galaxy rotation curves in extremely diffuse systems systematically deviate from the

predicted saturation behavior, the framework would require revision or rejection.

Conversely, the confirmation of environment-dependent expansion signatures or consistent saturation behavior across diverse galactic systems would provide strong support for the model.

#### 5.7 Summary

The effective saturation framework is robust against reasonable baryonic uncertainties and cannot be trivially absorbed into existing astrophysical or cosmological effects. Its explanatory power arises from the use of a single universal scale and from its explicit environmental dependence.

The framework is limited in scope but sharply testable. Its validity hinges on future observational probes of low-density environments, making it a falsifiable proposal rather than a flexible phenomenological fit.

### 6 PREDICTIONS AND OBSERVATIONAL TESTS

The effective saturation framework introduced in this work leads to a set of distinct and testable predictions. These predictions follow directly from the environmental dependence of the effective transition resolution and do not rely on additional assumptions or parameter tuning.

#### 6.1 Environment-Dependent Hubble Measurements

A primary prediction of the framework is a correlation between the locally inferred Hubble constant and the surrounding large-scale environment.

Observers and standard candles located in or near deep cosmic voids are expected to yield systematically higher inferred values of  $H_0$  than those located in denser regions. Conversely, measurements anchored in overdense environments should converge more closely toward the global expansion rate  $H_{\text{global}}$ .

This prediction can be tested by cross-correlating existing and forthcoming  $H_0$  measurements with void catalogs and density reconstructions derived from large-scale galaxy surveys, as already explored in the context of local underdensity scenarios [Keenan et al. \(2013\); Shanks \(2019\); Kenworthy et al. \(2019\)](#). A statistically significant null result would strongly disfavor the effective saturation mechanism.

In particular, the framework predicts a differential signal: measurements performed in environments of comparable redshift but contrasting large-scale density should exhibit systematically different inferred values of  $H_0$ .

#### 6.2 Redshift Dependence of the Hubble Offset

The environmental bias predicted by the framework is inherently scale dependent.

At sufficiently low redshift, local measurements are sensitive to individual large-scale structures and directly probe the saturated regime. At increasing redshift, line-of-sight averaging over multiple environments progressively suppresses the bias.

As a result, the inferred expansion rate is predicted to converge smoothly toward  $H_{\text{global}}$  with increasing redshift.

This behavior provides a clear observational signature. Measurements of the Hubble constant performed over different redshift ranges

should exhibit a systematic trend, with the largest deviations appearing at the lowest redshifts, followed by a gradual convergence at higher redshift [Verde et al. \(2019\)](#).

An important quantitative consequence of the framework is that the expected deviation remains at the percent level. Once the saturation scale  $a_*$  is fixed by galactic dynamics, the fractional offset in the inferred expansion rate is predicted to peak at intermediate redshift and to remain negligible at both very low and sufficiently high redshift.

The peak is expected when the typical line-of-sight length becomes comparable to the characteristic scale of large voids, before full environmental averaging sets in.

Such deviations fall within the sensitivity range of forthcoming large-scale surveys, including DESI and *Euclid*. Observed deviations significantly larger or smaller than this level would directly challenge the proposed mechanism.

### 6.3 Void-Specific Redshift Drift

The effective saturation mechanism also affects the temporal evolution of redshift for sources embedded in low-density environments.

In the standard cosmological framework, the redshift drift depends solely on the global expansion history. In the present framework, sources located in deep voids experience a modified effective transition rate, leading to a small but systematic deviation in the expected redshift drift signal.

Future high-precision spectroscopic experiments may be able to detect this effect by comparing sources located in voids with those in denser regions, complementing existing redshift-drift proposals [Cai et al. \(2017\)](#). The effect is predicted to be suppressed at high redshift, where environmental averaging dominates.

### 6.4 Weak Lensing Signatures in Voids

Because the effective framework modifies the inferred gravitational response in low-density regions, it also impacts weak gravitational lensing by cosmic voids.

The model predicts subtle but systematic deviations in void lensing profiles relative to standard expectations. In particular, the effective saturation leads to a systematically altered lensing efficiency compared to what would be inferred from baryonic matter alone, without invoking additional dark components.

Void lensing measurements therefore provide an independent probe of the framework, complementary to kinematic tests, and have been identified as sensitive diagnostics of gravitational behavior in underdense regions [Cai et al. \(2017\)](#).

### 6.5 Predictions for Ultra-Diffuse Galaxies

Ultra-diffuse galaxies constitute extreme low-surface-density systems and probe the saturated regime across most of their spatial extent [van Dokkum \(2016\)](#).

The effective saturation framework predicts that such systems should exhibit slowly rising or weakly varying rotation curves, approaching a common asymptotic behavior largely independent of detailed baryonic structure. Significant departures from this pattern would challenge the universality of the saturation scale.

Observations reveal a wide diversity of inferred dynamical mass content among ultra-diffuse galaxies, ranging from apparently dark-matter-rich systems to galaxies consistent with little or no dark matter [van Dokkum \(2019\); Mancera Piña \(2019\)](#). Within the present

framework, this diversity arises naturally from differences in how deeply individual systems probe the saturated regime.

In ultra-diffuse galaxies, the apparent mass discrepancy inferred from kinematics should therefore not be interpreted as evidence for an extended distribution of unseen matter. It reflects a geometric threshold effect. The baryonic configuration probes a regime in which further density dilution no longer increases the effective dynamical response.

As a result, the inferred dynamical mass tracks the onset of saturation rather than the presence of an additional gravitating component. The apparent “missing mass” is thus an emergent consequence of limited effective resolution in low-density systems.

This interpretation leads to a falsifiable prediction. If the inferred mass discrepancy originates from geometric saturation rather than from a material mass component, independent mass tracers should not reveal correspondingly extended matter distributions.

In particular, weak lensing signals, satellite dynamics, and stellar velocity dispersion profiles are expected to systematically underpredict the dynamical mass inferred from kinematic measurements in the deepest saturation regime. A positive detection of massive, spatially extended halos in ultra-diffuse galaxies would directly falsify the present framework.

Because ultra-diffuse galaxies probe the deepest saturation regime, they provide a particularly sensitive test of the universality of the saturation scale  $a_*$ .

### 6.6 Summary

The effective saturation framework yields a coherent and tightly constrained set of predictions across both galactic and cosmological scales.

All predictions arise from environmental dependence and involve no additional free parameters beyond the saturation scale  $a_*$  already fixed by rotation curve data.

The framework is therefore falsifiable with current or near-future observational capabilities. Confirmation or rejection of these signatures will decisively determine whether the proposed mechanism captures a genuine aspect of low-density gravitational phenomenology.

## 7 CONCLUSION

We have examined whether two long-standing observational anomalies, namely flat galaxy rotation curves and the Hubble constant tension, may originate from a common effective mechanism operating in low-density environments.

Using a minimal phenomenological framework characterized by a single saturation scale, we have shown that baryonic matter alone can reproduce the main features of observed galaxy rotation curves across a wide range of systems, without halo-by-halo tuning or the introduction of dark matter particles within this effective description. This conclusion is supported by direct comparisons with representative rotation curves from the SPARC sample.

The same effective mechanism extends naturally to cosmological low-density regions. Cosmic voids, which probe the deepest saturation regime, emerge as key laboratories for this framework. In these environments, the locally inferred expansion rate is predicted to deviate systematically from the global value inferred from early-universe observables, while the background cosmological evolution remains unchanged.

Crucially, the framework does not modify early-time physics, does

not alter the global expansion history, and does not claim universal validity across all regimes. Quantities such as gravitational acceleration and the Hubble parameter are interpreted as effective inference rates, not as fundamental dynamical fields.

A distinctive strength of the approach lies in its cross-sector falsifiability. Because the same saturation scale governs both galactic dynamics and environment-dependent expansion inference, observational constraints obtained in one sector directly restrict the allowed phenomenology in the other. In particular, measurements of ultra-diffuse galaxy kinematics, which probe the deepest saturation regime at galactic scales, place quantitative bounds on the magnitude of any environment-dependent offset in the inferred Hubble constant. Conversely, the absence of such an offset in cosmological observations would falsify the interpretation of galactic low-acceleration behavior as a saturation effect.

The strength of the framework thus lies not in fitting individual anomalies in isolation, but in tying together galactic and cosmological phenomenology through a single effective scale and a shared environmental dependence. This coherence sharply limits the available parameter space and prevents independent adjustment of the two sectors.

We have identified several observational tests capable of confirming or excluding the framework. These include correlations between inferred values of  $H_0$  and large-scale environment, redshift-dependent suppression of the local offset, void-specific redshift drift, weak lensing signatures, and the dynamics of ultra-diffuse galaxies.

Taken together, these results suggest that galaxy rotation curves and the Hubble tension may reflect a shared low-density phenomenology rather than independent failures of the standard cosmological model. Whether this effective description captures a genuine aspect of gravitational inference or represents an intermediate phenomenological layer will ultimately be decided by targeted observational tests in the coming years.

## DATA AVAILABILITY

The galaxy rotation-curve data used in this work are drawn from the publicly available SPARC database Lelli et al. (2016).

The numerical code used to generate the galaxy rotation-curve figures and associated diagnostics is openly available and archived with a persistent identifier. The version used in this work is available via Zenodo at <https://doi.org/10.5281/zenodo.18462369> Beau (2026d).

## ACKNOWLEDGEMENTS

The author acknowledges the use of large language models as an editorial and analytical assistant during manuscript preparation, including help with phrasing alternatives, consistency checks, and structured rewriting. All scientific claims, modelling choices, numerical results, and interpretations are the sole responsibility of the author.

## REFERENCES

- Beau J., 2026c, Preprint
- Beau J., 2026a, Preprint
- Beau J., 2026d, Cosmochrony Simulation Code: Cosmology and Rotation-Curve Pipeline, doi:10.5281/zenodo.18462369, <https://doi.org/10.5281/zenodo.18462369>
- Beau J., 2026b, Preprint
- Bekenstein J., Milgrom M., 1984, The Astrophysical Journal, 286, 7
- Cai Y.-C., Padilla N., Li B., 2017, MNRAS, 472, 4579
- Collaboration P., 2020, A&A, 641, A6
- Di Cintio A., Brook C. B., Dutton A. A., Macciò A. V., Stinson G. S., Knebe A., 2014, MNRAS, 441, 2986
- Famaey B., McGaugh S. S., 2012, Living Reviews in Relativity, 15, 10
- Freedman W. L., 2021, ApJ, 919, 16
- Keenan R. C., Barger A. J., Cowie L. L., 2013, ApJ, 775, 62
- Kenworthy W. D., Scolnic D., Riess A. G., 2019, ApJ, 875, 145
- Lelli F., McGaugh S. S., Schombert J. M., 2016, AJ, 152, 157
- Mancera Piña P. e. a., 2019, ApJ, 883, L33
- McGaugh S. S., Lelli F., Schombert J. M., 2016, Phys. Rev. Lett., 117, 201101
- Milgrom M., 1983, ApJ, 270, 365
- Riess A. G. e. a., 2022, ApJ, 934, L7
- Shanks T. e. a., 2019, MNRAS, 484, L64
- Verde L., Treu T., Riess A. G., 2019, Nature Astronomy, 3, 891
- Will C. M., 2014, Living Reviews in Relativity, 17, 4
- van Dokkum P. e. a., 2016, ApJ, 828, L6
- van Dokkum P. e. a., 2019, Nature Astronomy, 3, 1065